Journal of Nuclear Materials 392 (2009) 206–212

Contents lists available at ScienceDirect

Journal of Nuclear Materials

journal homepage: www.elsevier.com/locate/jnucmat

Performance of FCCI barrier foils for U–Zr–X metallic fuel

Ho Jin Ryu *, Byoung Oon Lee, Seok Jin Oh, Jun Hwan Kim, Chan Bock Lee

Recycled Fuel Development Division, Korea Atomic Energy Research Institute, 150 Deokjin-dong, Yuseong-gu, Daejeon 305-353, Republic of Korea

A B S T R A C T

Diffusion couple tests of U–Zr or U–Zr–Ce alloys vs. ferritic martensitic steels such as HT9 or T91 were carried out in order to evaluate the performance of the diffusion barrier candidates. Elemental metal foils of Zr, Nb, Ti, Mo, Ta, V and Cr were very effective in inhibiting interdiffusion between these fuels and steels. Eutectic melting between the fuels and steels was not observed in any of the diffusion couples using these diffusion barrier foils at annealing temperatures up to 800 °C. Among the metallic foils evaluated in this study, V and Cr exhibited the most promising performances as a diffusion barrier material for eliminating the fuel cladding chemical interaction problem. However, Zr, Nb and Ti showed an active interaction with the fuel mainly due to the large U solubility.

1. Introduction

Transuranic element (TRU) bearing metallic fuels are being developed for sodium-cooled fast reactors (SFR) in order to burn the long-lived fission products in spent nuclear fuel [1–3]. Because the experiences with TRU metallic fuel containing minor actinides are limited compared to U–Zr and U–Pu–Zr metallic fuels, the basic properties of a TRU fuel are currently being investigated extensively [4,5]. Fuel-cladding chemical interaction (FCCI) during irradiation can limit the performance of metallic fuel due to eutectic melting of the interaction products at temperatures much lower than the melting point of a fuel alloy [6]. Penetration of an interaction layer into the cladding also decreases the life of a fuel element because thinning of cladding by an interaction layer decreases the load bearing capability.

FCCI behavior of U–Zr and U–Pu–Zr alloys against Fe, Fe–Cr, D9 and HT9 have been investigated by out-of-pile annealing tests with diffusion couples [7–10]. Ferritic martensitic steels (FMS) such as HT9 and T91 are considered as candidate cladding materials for a SFR fuel due to their excellent irradiation performance [11]. Recently, a thin coating on the inside wall of cladding has been proposed to retard any interaction between the metallic fuel and its cladding [12,13]. Effectiveness of a Zr liner in mitigating pellet cladding interaction (PCI) for boiling water reactor (BWR) fuel is well established [14]. Crawford et al. fabricated a U–Pu–Zr fuel rod by injection casting into Zr sheath tubes [12]. When irradiated in the EBR-II up to 6 at.% burnup, the Zr-sheathed fuel showed good performance. Tokiwai et al. reported that the interdiffusion between U–Zr and HT9 was reduced when a ZrN layer or a V foil were formed on the HT9 cladding [12]. Keiser and Cole compared the out-of-pile diffusion couples tests of Zr or V disks against a 65U–19Pu–9Zr–2.5Mo–2.5Ru–2Nd alloy (compositions in wt%) [15]. V showed reduced interdiffusion with the U–Pu–Zr–Mo–Ru–Nd alloy compared to Zr at 700 °C.

There are many candidate materials for a diffusion barrier other than Zr and V. Refractory metals such as Nb, Mo and Ta have been widely used as diffusion barrier materials [16–18]. In this study, the diffusion barrier performances of various metallic layers were compared by out-of-pile diffusion couple tests. Zr, Nb, Ti, Mo, Ta, V and Cr foils were inserted between the U–Zr or U–Zr–Ce fuels vs. FMS to form diffusion couples and the microstructures of the diffusion couples after the annealing tests were analyzed.

2. Experimental procedures

Small rods of U–Zr and U–Zr–Ce alloys (U–Zr–X) were fabricated by induction melting of elemental U, Zr and Ce. Each rod was furnace-cooled after melting in zirconia crucibles. Nominal content of Zr was 10 wt% and the cerium content was 2 wt%. Ce was added to U–Zr in order to simulate lanthanide and minor actinide fission products. Disks of HT9 and T91 steels were used to simulate FMS cladding. Mechanical clamps of Type 304 stainless steel joined the diffusion couples which were vacuum sealed in quartz tubes as shown in Fig. 1.

Commercially available metallic foils of Zr, Nb, Ti, Mo, Ta, V and Cr were used as a diffusion barrier between the U–Zr–X and FMS. The thickness of the foils ranged from 20 to 30 μm and each foil was inserted between the U–Zr–X and FMS diffusion couples. Cr-coated HT9 disks were also produced using a plasma spray coating process. Cr powder of 30 μm average diameter was used for the plasma spray coating. Plasma gases were argon and hydrogen, the gas pressure was 25 kPa, the arc current was 630 A and the spray distance was 220 mm. The thickness of the plasma spray

* Corresponding author. Tel.: +82 42 868 8845; fax: +82 42 868 8824.
E-mail address: hjryu@kaeri.re.kr (H.J. Ryu).

0022-3115/$ - see front matter © 2009 Elsevier B.V. All rights reserved.
doi:10.1016/j.jnucmat.2009.03.011

Fig. 1. A photo showing vaccum-sealed stainless steel clamps containing a diffusion couple of U–Zr–X and FMS.

coated Cr layers was controlled to about 100 μm by multiple-pass coating.

Diffusion couple tests were conducted in a muffle furnace with annealing temperatures of 700–800 °C. Cross-sectional microstructures of the diffusion couple specimens were observed using a scanning electron microscope (SEM). The elemental composition of the interaction layers were measured using energy dispersive X-ray spectroscopy (EDS) and standardless quantitative data were obtained by the ZAF correction algorithm of the EDAX Genesis X-ray microanalysis software.

3. Results and discussion

Liquid phase formation in the diffusion couples can be identified by microstructural observation of the interaction layers. According to the experimental data for liquefaction of an interaction layer of U–10 wt%Zr/Fe, liquefaction occurs at about 725 °C [19]. A cross-sectional micrograph of a U–Zr–X vs. HT9 diffusion couple annealed at 700 °C for 96 h without diffusion barrier foils showed that various interaction phases were formed, as shown in Fig. 2(a). Keiser et al. characterized the interaction phases formed in U-Zr/HT9 diffusion couples annealed at 700 °C for 96 h [8]. Nakamura et al. also characterized the interaction phases formed in U–Zr/Fe–Cr diffusion couples annealed at 700 °C [10]. Among the phases formed in the interaction layers, UFe_2, U_6Fe and $ZrFe_2$ were the major phases according to their analyses. These phases are also observed in the interaction layers of U–Zr/HT9 diffusion couples in this study. In this study, HT9 and T91 steels were used at the same time and temperature, but there was little difference between the two steels in the observed interaction behavior for identical conditions.

Fig. 2(b) shows a scanning electron micrograph of the U–Zr/T91 diffusion couple annealed at 740 °C for 25 h. The microstructures of the interaction layers are different from those in Fig. 2(a). For example, the continuous UFe_2 layers on the U–Zr side observed in Fig. 2(a) are not shown in Fig. 2(b). Instead, a gray phase is dispersed in a brighter matrix in the interaction zone adjacent to T91, and a dark phase is dispersed in the interaction zone near to U–Zr. This microstructure is very similar to the U–Pu–Zr vs. Fe diffusion couple annealed at 650 °C [19]. Nakamura et al. reported that eutectic melting occurred at 650 °C because the Pu addition lowered the eutectic melting temperature of the interaction phases. According to a ternary phase diagram of U–Zr–Fe as shown in Fig. 3 [20,21], a liquid phase is formed at a composition in the range

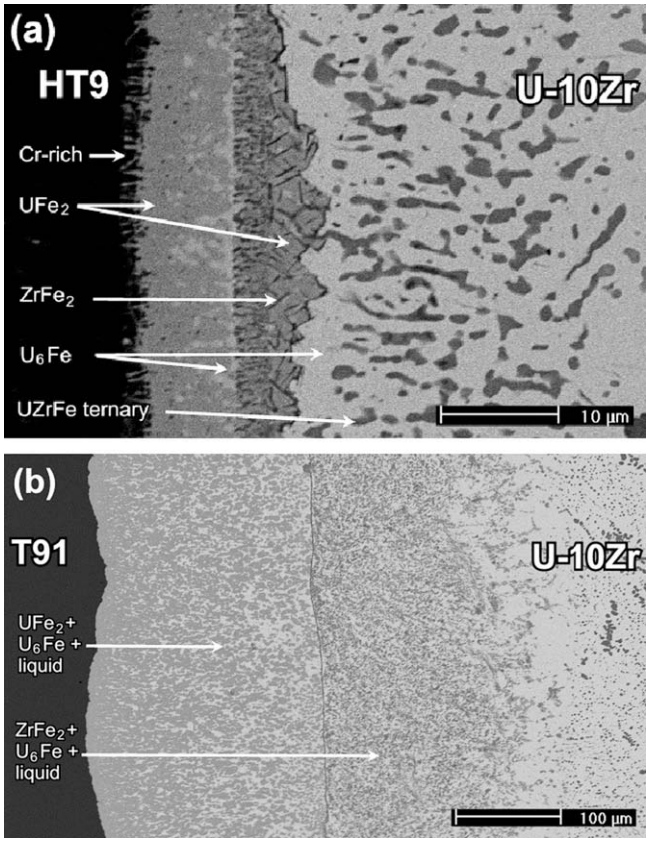

Fig. 2. Scanning electron micrographs of the interaction layers in: (a) a U–10Zr vs. HT9 diffusion couple annealed at 700 °C for 96 h and (b) a U–10Zr vs. T91 diffusion couple annealed at 740 °C for 25 h.

65–80 at.%U–Fe. The composition of the bright phase in the U–Zr side interaction zone in Fig. 2(b) was similar to the composition at which eutectic melting occurs in a ternary U–Zr–Fe.

When the annealing temperature was increased to 800 °C, eutectic-melted microstructures were observed as shown in Fig. 4(a) and they were much different from the layered structures formed below the eutectic temperature. The faceted dark phase was identified as $ZrFe_2$, the gray phase as UFe_2, and the bright matrix phase had the composition of a liquid phase as shown in Fig. 4(b). Average composition of the liquid phase was 60 at.%U–29 at.%Fe–8 at.%Cr–3 at.%Zr. One of the features in the eutectic-melted microstructure is that dark $ZrFe_2$ phases whose facets are well developed are distributed in a brighter matrix composed of around 60 at.%U and 30 at.%Fe.

In order to compare the diffusion barrier performances of metallic foils above the eutectic point of U–Zr–X vs. FMS, diffusion couples of U–Zr–Ce and a metallic foil were annealed at 740 °C for 25 h. Although, U–10 wt%Zr–2 wt%Ce alloy was used as a metallic fuel, any effect of Ce was not clearly shown in the microstructural analyses. It is believed that Ce was not dissolved in U–Zr and pure Ce particles were found in the U–Zr matrix as shown in Fig. 5. Fig. 6 shows the SEM micrographs after the diffusion couple tests using the metallic diffusion barriers at 740 °C for 25 h. The U–Zr–Ce side remained intact without eutectic melting with the diffusion barrier metals. However, many kinds of interactions were observed in the other diffusion couples using various metallic diffusion barriers. Dissolution of Zr-rich precipitates (UZr_2) was observed in the diffusion couples using Nb, Ti, Mo, Ta and V foils. Zr-rich precipitates were maintained only when Zr foils were used as shown in Fig. 6(a). Thickness of the diffusion barrier layers was increased from 23 to 33 μm in the diffusion couples using Zr. Multilayers

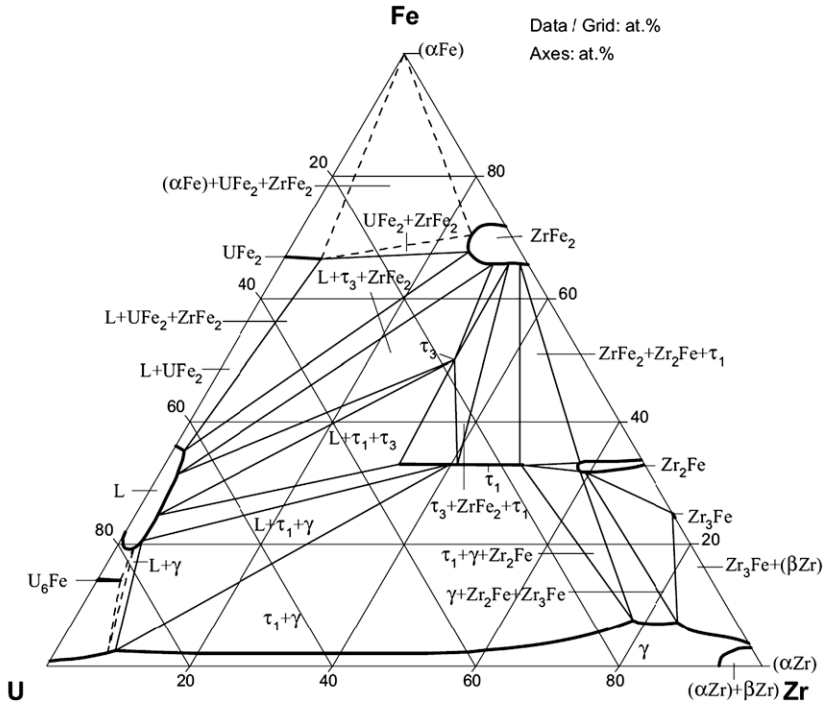

Fig. 3. An isothermal section of the ternary phase diagram of U–Zr–Fe at 800 °C [21].

were formed in the diffusion couples using Nb and Mo, as shown by the example for Nb in Fig. 6(b). Cr and V foils showed a minimum interaction in the diffusion couple test at 740 °C. Because the performance of the diffusion barrier foils was well characterized in the data from the 800 °C annealing tests, and will be presented below, characterization of the interaction layers for the 740 °C annealing tests are not presented in detail here.

From the binary phase diagrams of U and the candidate barrier metals tested in this study, the basic performance of the barrier metals can be estimated. Diffusion barrier metals should be chosen that do not

(a) have a large U solubility,
(b) form intermediate phases with U and
(c) have a lower eutectic melting temperature with U alloy.

Basic properties of the binary systems for the candidate diffusion barrier elements and uranium are summarized by their binary phase diagrams [22].

(a) V–U binary system has a eutectic point at 1040 °C. Solubility of U in V is lower than 4 wt% at around 800 °C. There is no intermediate phase in the V–U binary system.

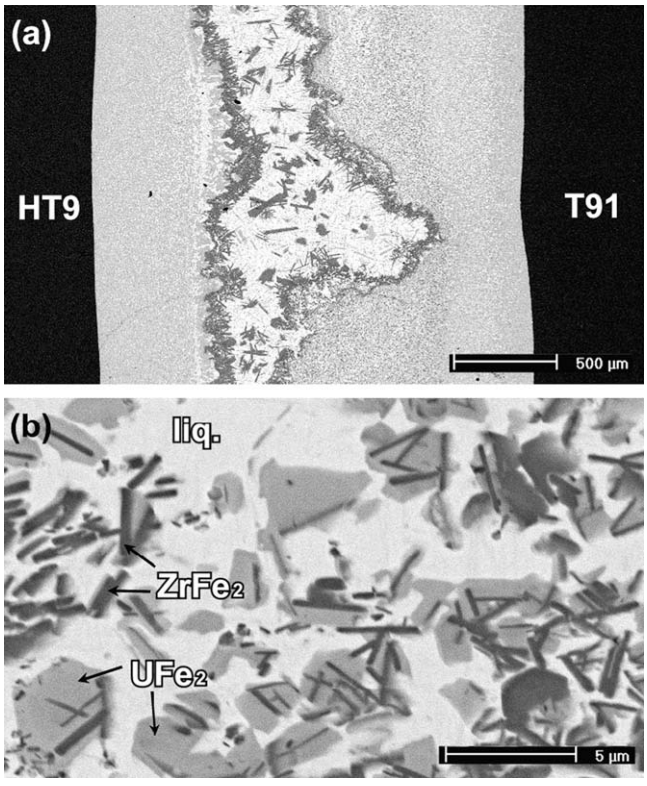

Fig. 4. Scanning electron micrographs of the diffusion couples of: (a) HT9/U–10Zr/T91 annealed at 800 °C for 7 h and (b) a magnified micrograph for the melted zone consisting of UFe_2 and $ZrFe_2$ in a liquid matrix.

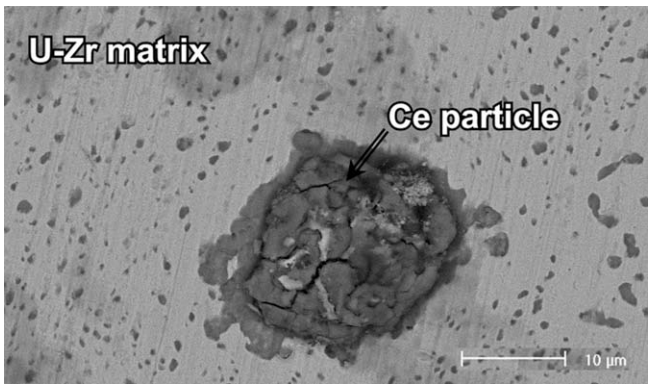

Fig. 5. A scanning electron micrograph of a pure Ce particle incorporated in a U–10Zr–2Ce alloy.

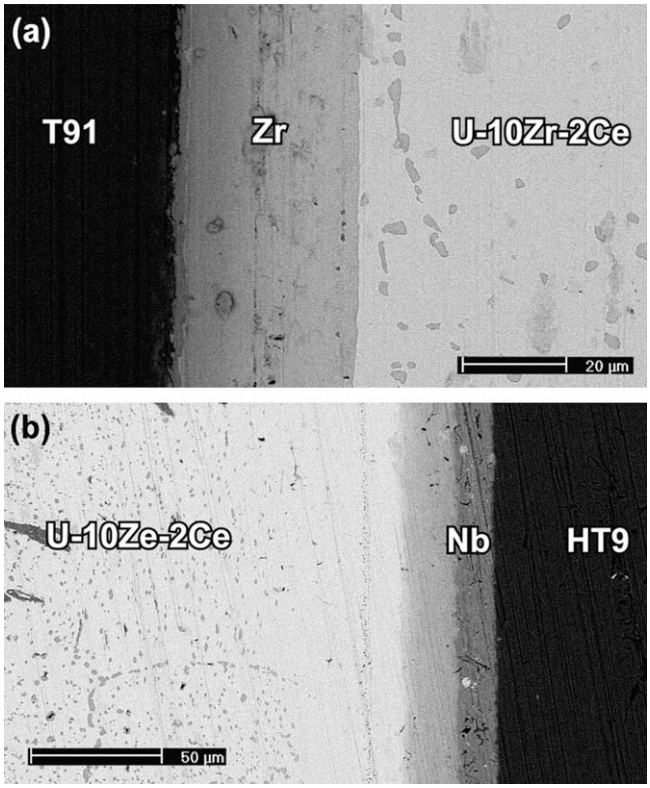

Fig. 6. Scanning electron micrographs of the diffusion couples of: (a) U–10Zr–2Ce and T91 with a Zr diffusion barrier and (b) U–10Zr–2Ce and HT9 with a Nb diffusion barrier, both annealed at 740 °C for 25 h.

(b) Cr–U binary system has a eutectic point at 860 °C. Solubility of U in Cr is very limited. There is no intermediate phase in the Cr–U binary system.
(c) Zr–U binary system has no eutectic reaction. γ-U and β-Zr form a perfect solid solution. There is a δ phase (UZr_2) in the Zr–U binary system.
(d) Ti–U binary system has no eutectic reaction. γ-U and β-Ti form a perfect solid solution. There is an U_2Ti phase in the Ti–U binary system.
(e) Mo–U binary system has no eutectic reaction. Solubility of U in Mo is very limited whereas the solubility of Mo in U is large at up to 40 at.%. There is a U_2Mo phase in the Mo–U binary system.
(f) Nb–U binary system has no eutectic point. γ-U and Nb form a perfect solid solution. There is no intermediate phase in the Nb–U binary system.
(g) Ta–U binary system has no eutectic reaction. Solubility of U in Ta and the solubility of Ta in U are very limited. There is no intermediate phase in the Ta–U binary system.

From the binary phase diagram analyses of the candidate metal elements with uranium, V, Cr and Ta appeared to offer good diffusion barrier performance against uranium. In contrast, Zr, Nb and Ti are expected to have poor diffusion barrier performance against uranium, because uranium has an unlimited solubility in them, which means interdiffusion occurs readily at their interface.

Diffusion barrier performances of the metallic foils were compared by diffusion couple annealing tests at 800 °C for 25 h. Annealing at 800 °C, which is much higher than the projected use temperature for metallic fuel, has triple purposes: first, it was to accelerate the interdiffusion for a performance comparison between the candidate barrier materials, second, it was to simulate a transient state, and third, it was to compensate for the missing Pu which lowers the melting temperature of metallic fuel alloys.

Fig. 7 shows the scanning electron micrographs of the cross-sections of the diffusion couples annealed at 800 °C for 25 h by using a Zr foil, a Nb foil and a Ti foil. The initial thickness of each foil is listed in Table 1. There remained no inert thicknesses of these foils due to their active interaction with U. Composition distribution of the constituent elements was measured by EDS. Zr-rich particles were observed commonly in the U–Zr side of the diffusion couples and some pores, shown as darker areas, were observed inside some barrier foils such as Nb, Ti, Ta and V.

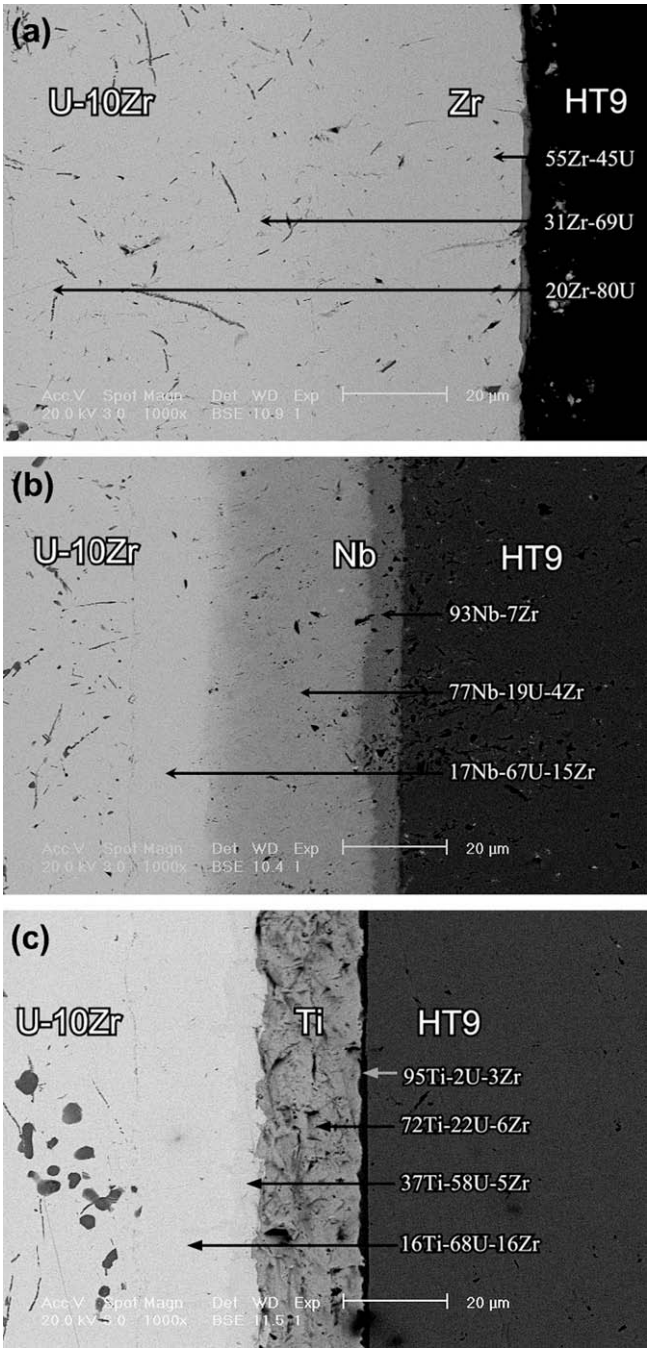

Fig. 7. Scanning electron micrographs of the diffusion couples of U–10Zr and HT9 with: (a) a Zr diffusion barrier, (b) a Nb diffusion barrier and (c) a Ti diffusion barrier, which were annealed at 800 °C for 25 h.

Table 1
Thickness changes for each barrier material after diffusion couple tests at 800 °C for 25 h.

Barrier materials	Initial thickness (μm)	Inert thickness after annealing (μm)
Zr	25	0
Nb	35	0
Ti	25	0
Mo	27	19
Ta	31	25
V	26	23
Cr	38	37

The Zr foil and U formed a solid solution. No elemental Zr remained after 25 h at 800 °C. The measured Zr content decreased from 55 to 20 at.% from the HT9 side to the U–Zr side, as shown in Fig. 7(a). Fig. 8 shows the composition profile of Zr and U along the distance from the Zr foil toward the U–Zr side. No distinct boundaries were found after diffusion couple annealing. A large amount of U, more than 40 at.%, penetrate into the initial Zr foil by interdiffusion. The Zr–U alloy at the interface can cause eutectic melting with FMS cladding if annealed longer than 25 h.

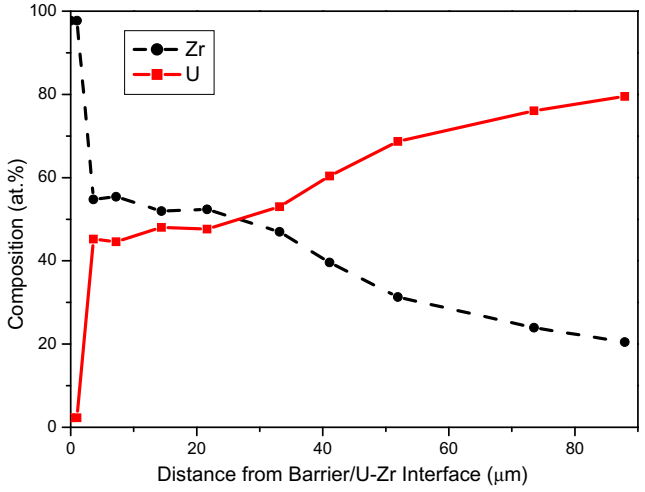

Fig. 8. Composition profiles of Zr and U along the distance from Zr foil toward the U–Zr side.

When an Nb foil was used, Nb and U–Zr formed a solid solution as shown in Fig. 7(b). The Nb and U–Zr formed three interaction layers of 67 at.%U–17 at.%Nb–15 at.%Zr, 77 at.%Nb–19 at.%U–4 at.%Zr and 93 at.%Nb–7 at.%Zr.

The Ti and U–Zr formed a solid solution in a diffusion couple using a Ti foil, as shown in Fig. 7(c). Composition of the Ti foil changed to Ti–22at.%U–6at.%Zr, and Ti also penetrated into the U–Zr side. An intermediate interaction layer similar to a TiU_2 phase was formed and its composition was measured as 37 at.%Ti–58 at.%U–5 at.%Zr. The δ phase precipitates in the U–Zr dissolved in the interaction zone near the Ti layer and the composition was 16 at.%Ti–68 at.%U–16 at.%Zr. The Zr, Ti and Nb interacted actively with U–Zr as predicted from the binary phase diagram study. Fig. 9 shows the phase formation in the U–Ti system at 800 °C. The four interaction phases expected to form in a U–Ti diffusion couple at 800 °C, are observed in the diffusion couple test using the Ti foil, Fig. 7(c).

Fig. 10 shows the scanning electron micrographs of the cross-sections of the diffusion couples annealed at 800 °C for 25 h using a Mo foil, a Ta foil and a V foil. The initial thickness and remained inert thickness of each foil are compared in Table 1. The thicknesses of the Mo foil and Ta foil were reduced from their initial thickness due to a small amount of interaction with U. Fig. 10(a) shows that a U–12 at.%Mo layer was formed on the Mo layer in the diffusion couple using the Mo foil. Although a pure Mo layer remained after a diffusion couple test at 800 °C for 25 h, Mo showed an active interaction with U–Zr and formed multiphase layers composed of U–Mo and Zr–Mo. When the Ta foil was used, a pure Ta layer remained and some Ta diffused into the U–Zr to form the ternary U–Zr–Ta phase as shown in Fig. 10(b). Fig. 10(c) shows that V and U did not react with each other because of their mutual insolubility. Elemental Zr formed a thin layer between U–Zr and V. No U was detected in the EDX analysis inside the V layer. A ternary V–Fe–Zr layer was observed between the V foils and the FMS showed the measured composition was 93.5 at.%V–4 at.%Fe–2.5 at.%Zr. The reduction of V foil thickness after annealing, as

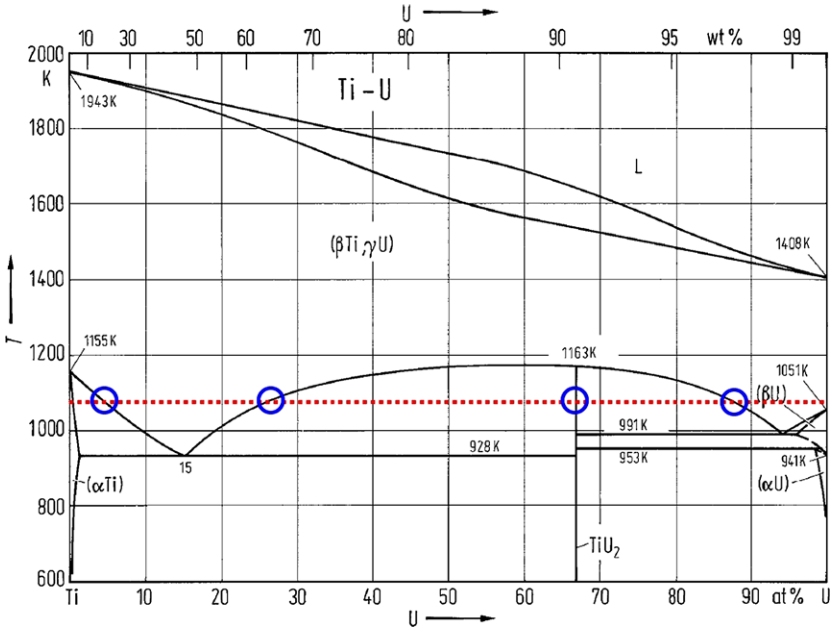

Fig. 9. A binary phase diagram of U–Ti system showing that four layers with circled compositions can be formed when annealed at 800 °C (dotted line) [22].

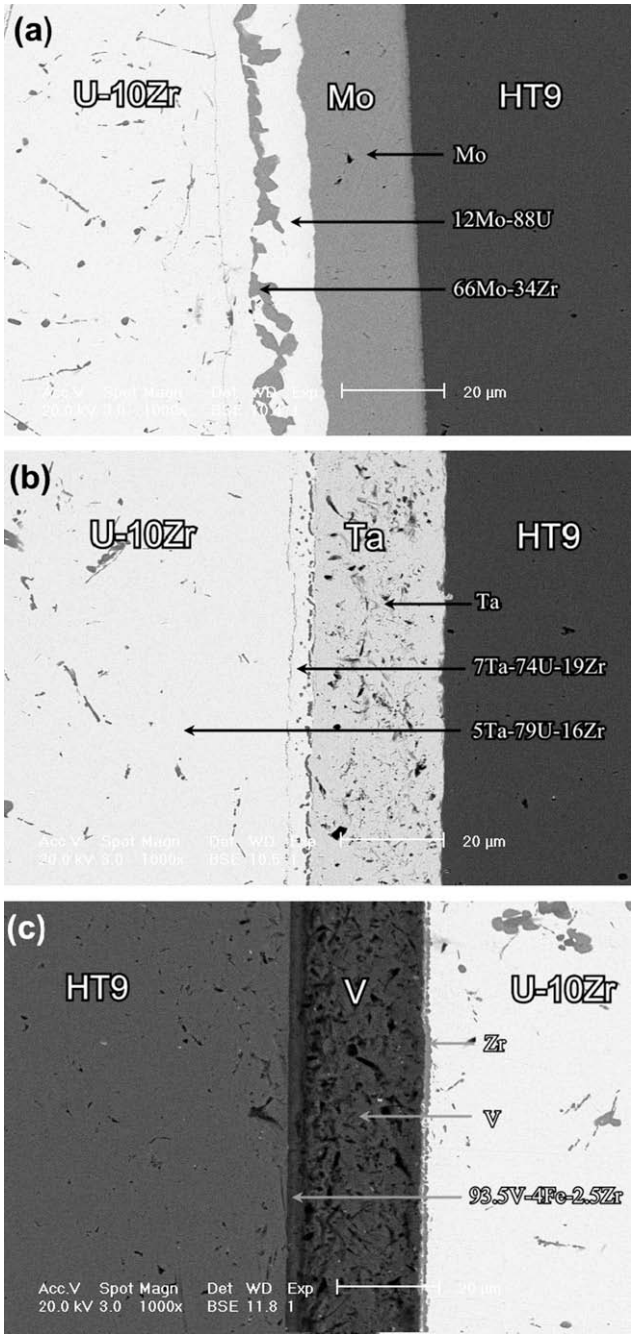

Fig. 10. Scanning electron micrographs of the diffusion couples of U–10Zr and HT9 with: (a) a Mo diffusion barrier, (b) a Ta diffusion barrier, and (c) a V diffusion barrier, which were annealed at 800 °C for 25 h.

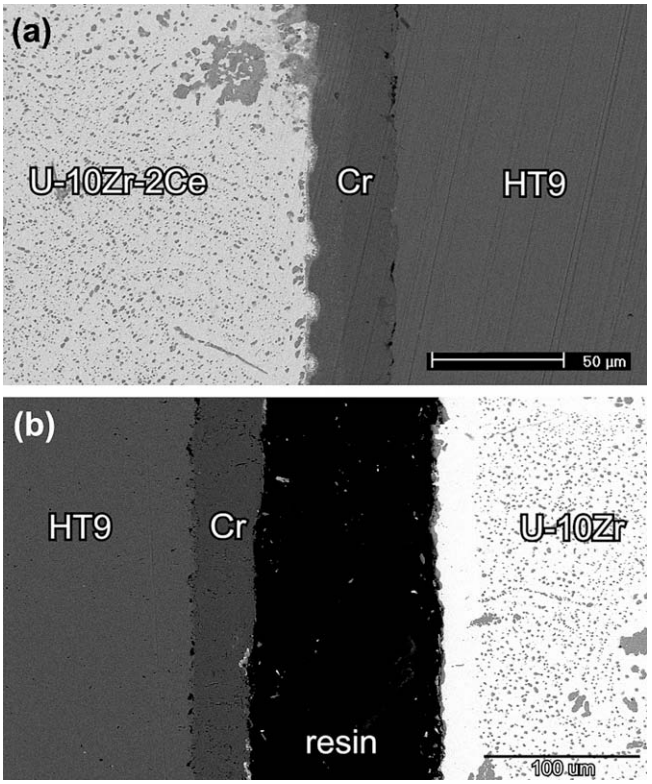

Fig. 11. Scanning electron micrographs of the diffusion couples of U–Zr–X and HT9 with: (a) a Cr diffusion barrier foil annealed at 740 °C for 25 h and (b) a plasma-sprayed Cr diffusion barrier coating annealed at 800 °C for 25 h.

shown in Table 1, is associated with the interaction between V and FMS.

Diffusion couple test at 740 °C also showed good diffusion barrier performance for a Cr foil. Fig. 11(a) shows that no interaction was observed between the U–Zr and Cr foil. Although the Cr foils were effectively located between the U–Zr and FMS in a diffusion couple test at 740 °C, the commercially available Cr foils were too brittle to be clamped between two disks as a single layer. The annealing test at 740 °C (Fig. 11(a)) is the only test using commercial Cr foil and we used plasma-sprayed Cr coatings in the annealing test at 800 °C (Fig. 11(b)). Cr and U–Zr did not react with each other and the elemental Cr remained after a 25 h diffusion couple test at 800 °C, when the thickness of Cr coating was 38 μm, as shown in Fig. 11(b). There was a minimal thickness change after a diffusion couple test using the Cr coating as listed in Table. 1.

The excellent diffusion barrier performance of V had been reported in the literature. Cohen et al. reported that V alloy cladding had excellent metallurgical compatibility with U–Pu–Zr alloys as compared to steel in in-reactor tests conducted by Argonne National laboratory in the 1960s [23]. Keiser and Cole reported that interdiffusion zone width for the U alloy/Zr diffusion couple is larger than for the U alloy/V when annealed at 700 °C for 75 h [15]. Tokiwai et al. reported that V foil showed good barrier performance in diffusion couple tests at both 750 °C for 2250 h and 750 °C 200 h plus 800 °C 1 h [13]. The inert interdiffusion behavior of V with U alloys, shown in this study, agreed well with the previous results.

However, little attention has been given to the diffusion barrier performance of Cr for metallic fuel cladding. One of significant results of this study is the promising performance of Cr as a diffusion barrier coating. Another significant result is the relatively poor diffusion barrier performance of Zr, although Zr has been considered to be a strong candidate for FCCI barrier material [12]. Use of Zr foils charged with nitrogen might increase the diffusion barrier performance of Zr because Tokiwai et al. showed that Zr foils charged with nitrogen blocked interdifusion of U and Fe due to formation of a very thin ZrN layer, although most Zr foils were dissolved into U–Zr fuel [13].

The effects of the lanthanide fission product elements on FCCI are not yet clearly understood [24]. In this study, tests with U–Zr–Ce showed no significant change in the diffusion couple tests. It is believed that the isolated Ce particles observed in the microstructures resulted due to their limited solubility in the U–Zr matrix. Further diffusion couple tests of the fission product

lanthanides vs. diffusion barrier candidates are necessary in order to clarify the effect of lanthanides on FCCI.

Fabrication processes should be developed to apply a diffusion barrier coating to fuel cladding tubes. Various coating methods are being studied to develop diffusion barrier coated cladding tubes. In addition, such a diffusion barrier coating should have good compatibility with the cladding materials, with little effect on the mechanical properties and it must be radiation resistant. Neutron economy and fission product activation of diffusion barrier materials should also be addressed further.

4. Summary

In order to overcome the FCCI problem and the eutectic melting of metallic fuel, candidate diffusion barrier materials were tested by diffusion couple annealing tests with commercial metallic foils. Diffusion couples of U–Zr–X vs. FMS incorporating metallic diffusion barrier foils showed that interdiffusion was inhibited effectively by the presence of thin foils of about 20∼30 μm even above the eutectic melting temperature of U–Zr alloys and FMS. Comparing the interactions between U–Zr–X and various diffusion barrier materials, it is concluded that an element with a limited solubility of U and no intermediate phases with U should be used as a diffusion barrier material. V and Cr showed good diffusion barrier performance during the diffusion couple tests. Although Ta and Mo blocked interdiffusion of U and Fe, they diffused into the fuel. Zr, Nb and Ti are not suitable barriers as they showed active interaction with U–Zr–X due to the large U solubility.

Acknowledgments

This study was supported by the National Nuclear R&D Program of the Ministry of Education, Science and Technology (MEST) of Korea. The authors would like to thank Professor Yo Seung Song (Korea Aerospace University) for providing plasma spray coated HT9 and T91 disks.

References

[1] D.C. Crawford, D.L. Porter, S.L. Hayes, J. Nucl. Mater. 371 (2007) 202.
[2] G.L. Hofman, L.C. Walters, T.H. Bauer, Progr. Nucl. Energy 31 (1997) 83.
[3] Y.I. Chang, Nucl. Eng. Technol. 39 (2007) 161.
[4] C.L. Trybus, J.E. Sanecki, S.P. Henslee, J. Nucl. Mater. 204 (1993) 50.
[5] M. Kurata, T. Inoue, C. Sari, J. Nucl. Mater. 208 (1994) 144.
[6] M. Kurata, K. Nakamura, T. Ogata, J. Nucl. Mater. 294 (2001) 123.
[7] D.D. Keiser Jr., M.A. Dayananda, J. Nucl. Mater. 200 (1993) 229.
[8] D.D. Keiser Jr., M.C. Petri, J. Nucl. Mater. 240 (1996) 51.
[9] T. Ogata, M. Kurata, K. Nakamura, A. Itoh, M. Akabori, J. Nucl. Mater. 250 (1997) 171.
[10] K. Nakamura, T. Ogata, M. Kurata, A. Itoh, M. Akabori, J. Nucl. Mater. 275 (1999) 246.
[11] R.L. Klueh, A.T. Nelson, J. Nucl. Mater. 371 (2007) 37.
[12] D.C. Crawford, C.E. Lahm, H. Tsai, R.G. Pahl, J. Nucl. Mater. 204 (1993) 157.
[13] M. Tokiwai, A. Kawabe, R. Yuda, T. Usami, R.H. Nakamura, H. Yahata, J. Nucl. Sci. Technol. (Suppl. 3) (2002) 917.
[14] B. Cox, J. Nucl. Mater. 172 (1990) 249.
[15] D. Keiser, J. Cole, GLOBAL-2007, Boise, Idaho, 9–13 September 2007.
[16] B.N. Briggs, W.H. Friske, NAA-SR-7973, Atomics International, 1962.
[17] A. He, D.G. Ivey, Mater. Sci. Eng. B 106 (2004) 33.
[18] M. Ahmad, J.I. Akhter, Q. Zaman, M.A. Shaikh, M. Akhtar, M. Iqbal, E. Ahmed, J. Nucl. Mater. 317 (2003) 212.
[19] K. Nakamura, T. Ogata, M. Kurata, T. Yokoo, M.A. Mignanelli, J. Nucl. Sci. Technol. 39 (2001) 112.
[20] K. Nakamura, M. Kurata, T. Ogata, A. Itoh, M. Akabori, J. Nucl. Mater. 275 (1999) 151.
[21] G. Effenberg, S. Ilyenko (Eds.), Ternary Alloy Systems, Landolt-Börnstein – Group IV Physical Chemistry, vol. 11C4, Springer, Berlin Heidelberg, 2007, p. 326.
[22] T.B. Massalski (Ed.), Binary Alloy Phase Diagrams, ASM International, 1990.
[23] A.B. Cohen, T.C. Wiencek, H. Tsai, in: Proceedings of 15th Conference on Advances in the Production of Tubes, Bars and Shapes, ASM International, Clearwater, FL, USA, 2–3 May 1994.
[24] C. Sari, C.T. Walker, M. Kurata, T. Inoue, J. Nucl. Mater. 208 (1994) 201.